

Backstepping Method and Control Allocation for a Fully-Actuated Tri-Rotor



Yunhe Wang, Zhangzhen Zhu, and Yu Zhang

Abstract This paper considers a tilting tri-rotor unmanned aerial vehicle (UAV) with each rotor having a tilting degree of freedom. The dynamic model of this UAV is obtained in this paper, which is a fully-actuated system instead of an underactuated system. Although it is not a redundant system, it also needs control allocator to distribute virtual control commands to actuators. Therefore, we propose a new control allocation method to solve this nonlinear problem. Meanwhile, the Backstepping method is used to build the entire control architecture. Finally, several simulation experiments are conducted to demonstrate our proposed method.

Keywords Fully-Actuated Tri-Rotor · Backstepping · Control allocation

1 Introduction

Unmanned aerial vehicles (UAV) have recently attracted more and more research attention due to their wide applications and many significant advantages over manned aircrafts. There are many research points about UAVs, especially control method and structure design. With respect to the former, UAVs have successfully employed several control algorithms. The classical PID [1] and the ADRC [2] have been successfully implemented in the quadrotors. The H-infinity control method and Backstepping method have also been introduced for controlling a helicopter [3], and a tricopter UAV [4], respectively. Some scholars even involve Lie theory and design controller on manifold $SO(3)$ to avoid the problem of singularity of Euler

Y. Wang · Z. Zhu · Y. Zhang (✉)

State Key Laboratory of Industrial Control Technology, College of Control Science and Engineering, Zhejiang University, Hangzhou 310027, China
e-mail: zhangyu80@zju.edu.cn

Y. Wang

e-mail: 21832137@zju.edu.cn

Z. Zhu

e-mail: 11832015@zju.edu.cn

© The Editor(s) (if applicable) and The Author(s), under exclusive license to Springer Nature Singapore Pte Ltd. 2022

L. Yan et al. (eds.), *Advances in Guidance, Navigation and Control*,
Lecture Notes in Electrical Engineering 644,
https://doi.org/10.1007/978-981-15-8155-7_156

1857

angles [5]. With respect to the structure, UAVs can be roughly classified into rotorcrafts, fixed-wings, and other UAVs. Rotorcrafts can take off and land vertically or hover at a fixed point, but they exhibit some problems such as poor endurance. Fixed-wings have higher endurance than rotorcrafts due to their flight mechanics, but lack hovering capability. Furthermore, many kinds of nonconventional UAVs have been presented to accomplish various tasks [6].

The classical quadrotor is an underactuated system, while the classical hexarotors and octorotors are still underactuated systems, which means the underactuated system is not changed into a fully-actuated or over-actuated system due to the added rotors. This is because the directions of all rotors are always the same, so that the rotor thrusts are linearly related. Therefore, increasing thrust direction of the rotor is a key factor in improving the maneuverability of the fuselage. In general, there are two common methods. First, some scholars configure each rotor and guarantee the orientations of them are different [7]. Andrea proposed a parameter that represents the fuselage's agility and obtained the optimal rotors' orientation combination through trying different rotor orientation combinations to maximize the agility parameter. Second, several rotors are given one or two degrees of freedom to tilt, so that the rotor thrust vector can be changed within a certain range. This idea comes from the concept of thrust vectoring [8, 9]. This paper adopts the latter idea and considers a tilting tri-rotor, so that the system changes from underactuated to fully-actuated because of the given tilting degree of freedom (DOF). The fully-actuated system has the same number of control inputs and control outputs. Since each rotor has a tilt angle, the control allocation equation is nonlinear. Control allocation process maps virtual control commands generated from the controller into actuator commands that provide actual control efforts. The mapping from the virtual control commands to actuator commands is a one-to-one mapping for the fully-actuated system [10].

Generally, we divide control allocation into non-optimal control allocation and optimal control allocation based on whether or not optimization targets are considered. Our control allocation method is non-optimal. The system always can be described as follows:

$$\dot{\mathbf{x}} = f(\mathbf{x}, t) + g(\mathbf{x}, t)\mathbf{u}, \mathbf{y} = l(\mathbf{x}, t) \quad (1)$$

\mathbf{u} is the control input, \mathbf{x} is the state variable and \mathbf{y} is the output variable. As for a fully-actuated system, the common basic control allocation problem statement is expressed as: $\mathbf{u} = h(\mathbf{x}, \boldsymbol{\tau}, t)$, $\boldsymbol{\tau}$ is the actuator variable and we need to find an inverse transform: $\boldsymbol{\tau} = h^{-1}(\mathbf{x}, \mathbf{u}, t)$. However, most control allocation methods are based on a linear model, i.e.,

$$\mathbf{u} = h(\mathbf{x}, \boldsymbol{\tau}, t) = B(\mathbf{x}, t)\boldsymbol{\tau} \quad (2)$$

and $\boldsymbol{\tau} = B^{-1}(\mathbf{x}, t)\mathbf{u}$. Sometimes, the actuators' models are nonlinear like the model discussed in this paper. In the nonlinear case, we must analyze each specific problem

without a general nonlinear allocation algorithm. Herein, we present a new control allocation method, i.e. a new inverse mapping to attempt to tackle the nonlinear problem.

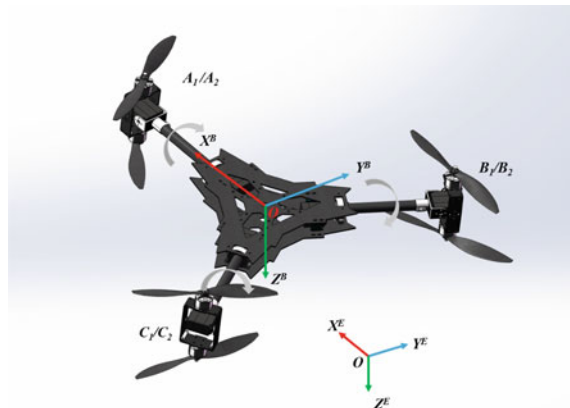
The remainder of the paper is organized as follows. The fuselage dynamic model is obtained in Sect. 2. Second, the entire control architecture is discussed in Sect. 3, and a Backstepping controller is introduced. This model has six controllable variables; therefore, the system is fully-actuated. A new control allocation method is proposed to form the whole control framework. Section 4 presents and discusses the results of simulation experiments. Finally, the conclusions are presented in Sect. 5.

2 Modeling

2.1 Structure of the UAV

Classical rotorcrafts, such as tri-rotors and quadrotors, must be tilted first in order to generate the component force in the horizontal direction, and then the fuselage is pushed forward, if an UAV wants to move in the horizontal direction. This way of moving forward is obviously inefficient and restrictive because there are more motion DOFs than controllable inputs in these classical models, i.e. the underactuated systems. In order to deal with this limit, each pair of coaxial rotors in the classical tri-rotor is given a tilting degree in this study. The specific model structure is shown in Fig. 1.

Fig. 1 Structure of the proposed tilting tri-rotor UAV



2.2 Description of the Dynamic Model

The coordinate system is defined as follows: the ground coordinate system $Ox^E y^E z^E$ and the body coordinate system $Ox^B y^B z^B$ are both set up as shown in Fig. 1. Herein, the ground coordinate system is considered as an inertial coordinate system. Moreover, in order to ignore the several subordinate factors, we employ the following assumptions: first, the effects of air resistance and wind are not considered, and the fuselage is considered as a rigid body; second, the moment of inertia tensor is a diagonal matrix to simplify the problem. Meanwhile, to prevent the tilting rotors from hitting the shafts, we limit the tilt angles. Specifically, the tilting angles range from: $\delta_i \in [\delta_{min}, \delta_{max}]$. The specific values of δ_{min} and δ_{max} are set in Sect. 4.

Based on these assumptions, the mechanics theory can be employed. According to the Newton-Euler formalism of rigid body and mechanics theories, we obtain the following formula [11]:

$$\begin{bmatrix} mI_{3 \times 3} & O_{3 \times 3} \\ O_{3 \times 3} & I \end{bmatrix} \begin{bmatrix} \dot{V}^B \\ \dot{\omega}^B \end{bmatrix} + \begin{bmatrix} \omega^B \times (mV^B) \\ \omega^B \times (I\omega^B) \end{bmatrix} = \begin{bmatrix} F^B \\ M^B \end{bmatrix}, \tag{3}$$

where $m, I = [I_x, I_y, I_z]$, $V^B = [u, v, w]$, $\omega^B = [p, q, r]$ are the mass, second-order moment of the inertia tensor of the fuselage, velocity and angular velocity in the body coordinate system of the UAV, respectively, and $F^B = [X_F, Y_F, Z_F]$, $M^B = [L, M, N]$ are the external force and external torque in the body coordinate system, respectively. Equation (3) can be expanded as follows:

$$\begin{cases} m\dot{u} = -mg \sin \theta + mr v - mq w + X_F \\ m\dot{v} = mg \cos \theta \sin \phi - mr u + mp w + Y_F \\ m\dot{w} = mg \cos \theta \cos \phi + mq u - mp v + Z_F \end{cases} \begin{cases} I_x \dot{p} = (I_y - I_z)qr + L \\ I_y \dot{q} = (I_z - I_x)rp + M \\ I_z \dot{r} = (I_x - I_y)pq + N \end{cases}. \tag{4}$$

where ϕ, θ, ψ are the Euler angles, and X_F, Y_F, Z_F, L, M, N are given as,

$$\begin{aligned} & [X_F \ Y_F \ Z_F \ L \ M \ N]^T \\ &= \frac{1}{2} \begin{bmatrix} 0 & 2s\delta_1 & -2c\delta_1 & 0 & 2lc\delta_1 & 2ls\delta_1 \\ -\sqrt{3}s\delta_2 & -s\delta_2 & -2c\delta_2 & -\sqrt{3}lc\delta_2 & -lc\delta_2 & 2ls\delta_2 \\ \sqrt{3}s\delta_3 & -s\delta_3 & -2c\delta_3 & \sqrt{3}lc\delta_3 & -lc\delta_3 & 2ls\delta_3 \end{bmatrix}^T \begin{bmatrix} F_1 \\ F_2 \\ F_3 \end{bmatrix}. \end{aligned} \tag{5}$$

Furthermore, according to [11], the conversion relationship between $[p, q, r]$ and $[\dot{\phi}, \dot{\theta}, \dot{\psi}]$, $[u, v, w]$ and $[\dot{x}, \dot{y}, \dot{z}]$ can be obtained as follows:

$$[\dot{\phi} \ \dot{\theta} \ \dot{\psi}]^T = \begin{bmatrix} 1 & \sin \phi \tan \theta & \cos \phi \tan \theta \\ 0 & \cos \phi & -\sin \phi \\ 0 & \sin \phi / \cos \theta & \cos \phi / \cos \theta \end{bmatrix} \begin{bmatrix} p \\ q \\ r \end{bmatrix}, \tag{6}$$

$$\begin{bmatrix} \dot{x} \\ \dot{y} \\ \dot{z} \end{bmatrix} = \begin{bmatrix} c\theta c\psi & c\psi s\theta s\phi - c\phi s\psi & s\phi s\psi + s\theta c\phi c\psi \\ c\theta s\psi & s\psi s\theta s\phi + c\phi c\psi & s\theta c\phi s\psi - s\phi c\psi \\ -s\theta & s\phi c\theta & c\phi c\theta \end{bmatrix} \begin{bmatrix} u \\ v \\ w \end{bmatrix}. \tag{7}$$

The ‘c’ represents ‘cos’, and the ‘s’ represents ‘sin’. (Same as below). The x, y, z are the coordinates of the fuselage centroid in the inertial system.

3 Control Architecture

The proposed system is fully-actuated, but the control allocation equation is nonlinear, which means conventional linear allocation methods are no longer applicable to proposed UAV. Therefore, this study comes up with a new control allocation method to design the control framework. Meanwhile, the control law involves the multiple inputs-multiple outputs (MIMO) Backstepping method. Overall, we want to make the proposed UAV successfully track the position and attitude targets by using corresponding control method and proposed control allocation method.

3.1 Backstepping Control Method

Considering the characteristics of Backstepping method, we first make an assumption here: the attitude angles of the body change within a small range, which means $\phi \approx 0, \theta \approx 0, \psi \approx 0$. Without this assumption, the calculation of the Backstepping method becomes very complicated. Under this assumption, our dynamic model is formed as:

$$\begin{cases} m\ddot{x} = X_F c\theta c\psi + Y_F(c\psi s\theta s\phi - c\phi s\psi) + Z_F(s\phi s\psi + s\theta c\phi c\psi) \\ m\ddot{y} = X_F c\theta s\psi + Y_F(s\psi s\theta s\phi + c\phi c\psi) + Z_F(s\theta c\phi s\psi - s\phi c\psi) , \\ m\ddot{z} = -X_F s\theta + Y_F s\phi c\theta + Z_F c\phi c\theta + g \end{cases} \tag{8}$$

$$\begin{cases} I_x \ddot{\phi} = (I_y - I_z) \dot{\theta} \dot{\psi} + L \\ I_y \ddot{\theta} = (I_z - I_x) \dot{\phi} \dot{\psi} + M . \\ I_z \ddot{\psi} = (I_x - I_y) \dot{\phi} \dot{\theta} + N \end{cases} \tag{9}$$

First, the model equation is written as the standard state space form as follows:

$$\dot{X} = f(X, U) = \begin{bmatrix} x_2 \\ a_1x_4x_6 + b_1U_4 \\ x_4 \\ a_2x_2x_6 + b_2U_5 \\ x_6 \\ a_3x_2x_4 + b_3U_6 \\ x_8 \\ U_1m^{-1}cx_3cx_5 + U_2m^{-1}(cx_5sx_3sx_1 - cx_1sx_5) + \\ U_3m^{-1}(sx_1sx_5 + sx_3cx_1sx_5) \\ x_{10} \\ U_1m^{-1}cx_3sx_5 + U_2m^{-1}(sx_5sx_3sx_1 - cx_1cx_5) + \\ U_3m^{-1}(sx_3cx_1sx_5 + sx_1cx_5) \\ x_{12} \\ -U_1m^{-1}sx_3 + U_2m^{-1}sx_1cx_3 + U_3m^{-1}cx_1cx_3 + g \end{bmatrix} = \begin{bmatrix} x_2 \\ a_1x_4x_6 + b_1U_4 \\ x_4 \\ a_2x_2x_6 + b_2U_5 \\ x_6 \\ a_3x_2x_4 + b_3U_6 \\ x_8 \\ f_1(U_1, U_2, U_3) \\ x_{10} \\ f_2(U_1, U_2, U_3) \\ x_{12} \\ f_3(U_1, U_2, U_3) \end{bmatrix}, \quad (10)$$

where $X = [\phi \ \dot{\phi} \ \theta \ \dot{\theta} \ \psi \ \dot{\psi} \ x \ \dot{x} \ y \ \dot{y} \ z \ \dot{z}]^T = [x_1, \dots, x_{12}]^T, a_1 = (I_y - I_z)/I_x,$
 $a_2 = (I_z - I_x)/I_y, a_3 = (I_x - I_y)/I_z, b_1 = I_x^{-1}, b_2 = I_y^{-1}, b_3 = I_z^{-1},$

$$U = [X_F, Y_F, Z_F, L, M, N]^T = [U_1, \dots, U_6]^T$$

Then, we consider attitude control, and we take ϕ as an example:

$$\begin{cases} \dot{x}_1 = x_2 \\ \dot{x}_2 = a_1x_4x_6 + b_1U_4 \end{cases}$$

We choose the Lyapunov candidate $V_1 = z_1^2/2$, where $z_1 = x_1 - x_{1d}$ and x_{1d} is the desired target. We define virtual command α_1 and $z_2 = x_2 - \alpha_1$, so we have:

$$\dot{V}_1 = z_1\dot{z}_1 = z_1(\dot{x}_1 - \dot{x}_{1d}) = z_1(x_2 - \dot{x}_{1d}) = z_1(z_2 + \alpha_1 - \dot{x}_{1d}).$$

We attempt to make \dot{V}_1 be negative definite, so we choose $\alpha_1 = \dot{x}_{1d} - c_1z_1$ ($c_1 > 0$), and

$$\dot{V}_1 = z_1\dot{z}_1 = -c_1z_1^2 + z_1z_2 \quad z_2 = x_2 - \alpha_1 = x_2 - \dot{x}_{1d} + c_1z_1.$$

We cannot recognize whether item z_1z_2 positive definite or not, so we need to further design it. We choose Lyapunov candidate $V_2 = z_2^2/2 + V_1 = z_1^2/2 + z_2^2/2$, and we have:

$$\begin{aligned} \dot{V}_2 &= z_1\dot{z}_1 + z_2\dot{z}_2 = z_2(\dot{x}_2 - \ddot{x}_{1d} + c_1\dot{z}_1) - c_1z_1^2 + z_1z_2 \\ &= z_2(a_1x_4x_6 + b_1U_4 - \ddot{x}_{1d} + c_1(z_2 - c_1z_1)) - c_1z_1^2 + z_1z_2. \end{aligned}$$

Therefore, we can choose

$$b_1U_4 = \ddot{x}_{1d} + (c_1^2 - 1)z_1 - a_1x_4x_6 - (c_1 + c_2)z_2, \dot{V}_2 = -c_1z_1^2 - c_2z_2^2 < 0 \quad (c_2 > 0)$$

[12, 13].

According to the Lyapunov’s theory, we know that control law U_4 can guarantee z_1, z_2 are asymptotically stable. In the same way, we can obtain the expressions of the control law U_5, U_6 as follows:

$$\begin{cases} U_4 = b_1^{-1} [\ddot{x}_{1d} + (c_1^2 - 1)z_1 - a_1x_4x_6 - (c_1 + c_2)z_2] \\ U_5 = b_2^{-1} [\ddot{x}_{3d} + (c_3^2 - 1)z_3 - a_2x_2x_6 - (c_3 + c_4)z_4] \\ U_6 = b_3^{-1} [\ddot{x}_{5d} + (c_5^2 - 1)z_5 - a_3x_2x_4 - (c_5 + c_6)z_6] \end{cases}, \tag{11}$$

where $c_i > 0$; $z_{2i-1} = x_{2i-1} - x_{(2i-1)d}$, $z_{2i} = x_{2i} - \dot{x}_{(2i)d} + c_{2i-1}z_{2i-1}$ ($i = 1, 2, 3$). Finally, we employ the Backstepping method to tackle with the position control.

Like the (11), we have:

$$\begin{cases} f_1(U_1, U_2, U_3) = \ddot{x}_{7d} + (c_7^2 - 1)z_7 - (c_7 + c_8)z_8 \\ f_2(U_1, U_2, U_3) = \ddot{x}_{9d} + (c_9^2 - 1)z_9 - (c_9 + c_{10})z_{10} \\ f_3(U_1, U_2, U_3) = \ddot{x}_{11d} + (c_{11}^2 - 1)z_{11} - (c_{11} + c_{12})z_{12} \end{cases}. \tag{12}$$

It’s obviously different from the attitude control equation. The three control variables U_1, U_2, U_3 are coupled in the three equations, so we cannot get them separately. We need to solve this system of ternary equations. The solution results of U_1, U_2, U_3 are also very complicated, since the forms of f_1, f_2, f_3 are complicated. Therefore, we do not show the specific expression of the control law U_1, U_2, U_3 here.

3.2 Control Allocation

According to (11) and (12), we have obtained the expression of the control law U_i . Next, we should distribute the control law to specific actuators, which is called control allocation. In this study, the control allocation equation is described as follows:

$$\begin{aligned} & [U_1 \ U_2 \ U_3 \ U_4 \ U_5 \ U_6]^T \\ &= \frac{1}{2} \begin{bmatrix} 0 & 2s\delta_1 & -2c\delta_1 & 0 & 2lc\delta_1 & 2ls\delta_1 \\ -\sqrt{3}s\delta_2 & -s\delta_2 & -2c\delta_2 & -\sqrt{3}lc\delta_2 & -lc\delta_2 & 2ls\delta_2 \\ \sqrt{3}s\delta_3 & -s\delta_3 & -2c\delta_3 & \sqrt{3}lc\delta_3 & -lc\delta_3 & 2ls\delta_3 \end{bmatrix}^T \begin{bmatrix} F_1 \\ F_2 \\ F_3 \end{bmatrix}. \end{aligned} \tag{13}$$

The $[U_1 \dots U_6]^T$ is three components of external forces and three components of external moments, respectively, and (13) is derived from mechanical analysis. Firstly, (13) must be simplified to illustrate the core problem. In fact, (13) can be denoted as follows [14]:

$$\begin{aligned} f_0 &= F_1 \sin \delta_1, \ b_0 = F_2 \sin \delta_2, \ d_0 = F_3 \sin \delta_3, \\ g_0 &= F_1 \cos \delta_1, \ h_0 = F_2 \cos \delta_2, \ m_0 = F_3 \cos \delta_3 \end{aligned} \tag{14}$$

Equation (14) is substituted into (13), giving

$$\begin{bmatrix} U_1 \\ U_2 \\ U_3 \\ U_4 \\ U_5 \\ U_6 \end{bmatrix} = \frac{1}{2} \begin{bmatrix} -\sqrt{3} & \sqrt{3} & 0 & 0 & 0 & 0 \\ -1 & -1 & 2 & 0 & 0 & 0 \\ 0 & 0 & 0 & -2 & -2 & -2 \\ 0 & 0 & 0 & 0 & -\sqrt{3} & \sqrt{3}l \\ 0 & 0 & 0 & l & -l & -l \\ l & l & l & 0 & 0 & 0 \end{bmatrix} \begin{bmatrix} b_0 \\ d_0 \\ f_0 \\ g_0 \\ h_0 \\ m_0 \end{bmatrix}. \tag{15}$$

The above equation group is solved to give

$$\begin{bmatrix} b_0 \\ d_0 \\ f_0 \\ g_0 \\ h_0 \\ m_0 \end{bmatrix} = \frac{1}{3} \begin{bmatrix} -\sqrt{3} & -1 & 0 & 0 & 0 & l^{-1} \\ \sqrt{3} & -1 & 0 & 0 & 0 & l^{-1} \\ 0 & 2 & 0 & 0 & 0 & l^{-1} \\ 0 & 0 & -1 & 0 & 2l^{-1} & 0 \\ 0 & 0 & -1 & -\sqrt{3}l^{-1} & -l^{-1} & 0 \\ 0 & 0 & -1 & \sqrt{3}l^{-1} & -l^{-1} & 0 \end{bmatrix} \begin{bmatrix} U_1 \\ U_2 \\ U_3 \\ U_4 \\ U_5 \\ U_6 \end{bmatrix}. \tag{16}$$

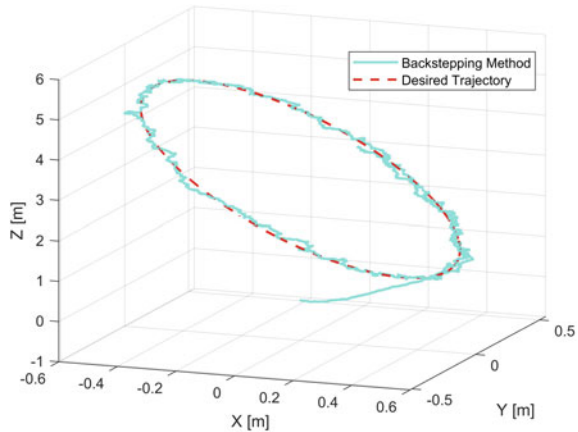
Meanwhile, it is worth noting here that F_i, δ_i can be determined after obtaining the parameters $b_0, d_0, f_0 \dots$. Only the following equations are required:

$$\begin{cases} F_1 = \sqrt{f_0^2 + g_0^2} \\ F_2 = \sqrt{b_0^2 + h_0^2} \\ F_3 = \sqrt{d_0^2 + m_0^2} \end{cases} \begin{cases} \delta_1 = \arcsin f_0/\sqrt{f_0^2 + g_0^2} \\ \delta_2 = \arcsin b_0/\sqrt{b_0^2 + h_0^2} \\ \delta_3 = \arcsin d_0/\sqrt{d_0^2 + m_0^2} \end{cases}. \tag{17}$$

4 Simulation

This simulation program is developed with the obtained conclusions. Every task is hard for classical rotorcrafts to conduct in each simulation, which corroborates the special advantages of this UAV. The detailed model parameters are shown as follows: the distance from centroid to rotor l is 0.41 m, the moment of inertia on the X, Y, Z axis I_x, I_y, I_z are 0.115 kgm², 0.115 kgm², 0.230 kgm², respectively. The mass of UAV m is 1.5 kg, and $\delta_i \in [-\pi/2, \pi/2]$. Meanwhile, 0.001 times Gaussian noise ($\mu = 0; \sigma^2 = 1$) is added into first simulation to increase the reliability of the simulation results.

Fig. 2 Spatial trajectory of the UAV of Exp1: Spatial ellipse with horizontal attitude (with noise)



4.1 Spatial Trajectory with Horizontal Attitude

In this simulation, the UAV tracks the spatial trajectory with horizontal attitude. Obviously, the conventional rotorcrafts must tilt its attitude first when moving horizontally, so they cannot accomplish this task. The initial position and attitude are $(0, 0, 0)$ m and $(0, 0, 0)$ rad, respectively. The desired attitude is $(0, 0, 0)$ rad, and the desired position is: $x_d = (0.5 \cos 0.05\pi t)$ m, $y_d = (0.5 \sin 0.05\pi t)$ m, $z_d = (3 - 2 \cos 0.05\pi t)$ m. The control coefficient $c_1 \sim c_6 = 10$, $c_7 \sim c_{12} = 4$. Figure 2 presents the fuselage spatial trajectory and Fig. 3 and 4 show the x, y, z coordinates and three attitude angles ϕ, θ, ψ , respectively.

Exp 1 demonstrates that this UAV can hold horizontal attitude during tracking a spatial trajectory by using Backstepping method, while the classical rotorcrafts cannot conduct this task because when it maintains horizontal attitude, there is no horizontal force component. At the same time, it can be seen that the robustness of this method is limited, and this method can only tolerate small amplitude errors. This is a disadvantage of this control method.

4.2 Zigzag with Horizontal Attitude by Applying Backstepping or PID

In this simulation, the UAV zigzags with horizontal attitude. We set the initial position and attitude are $(0, 0, 0)$ m and $(0, 0, 0)$ rad, respectively. The desired attitude is $(0, 0, 0)$ rad, and the desired trajectory is presented as follows:

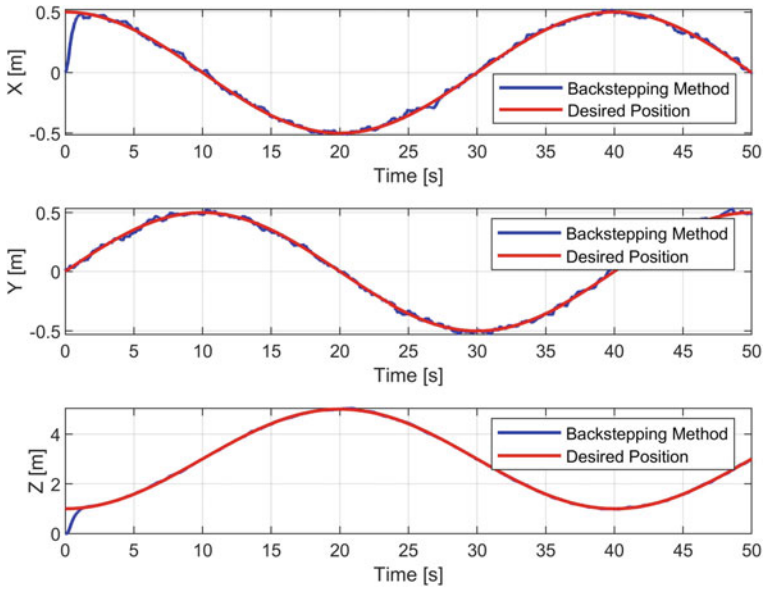


Fig. 3 Position of the UAV of Exp1: Spatial el-lipse with horizontal attitude (with noise)

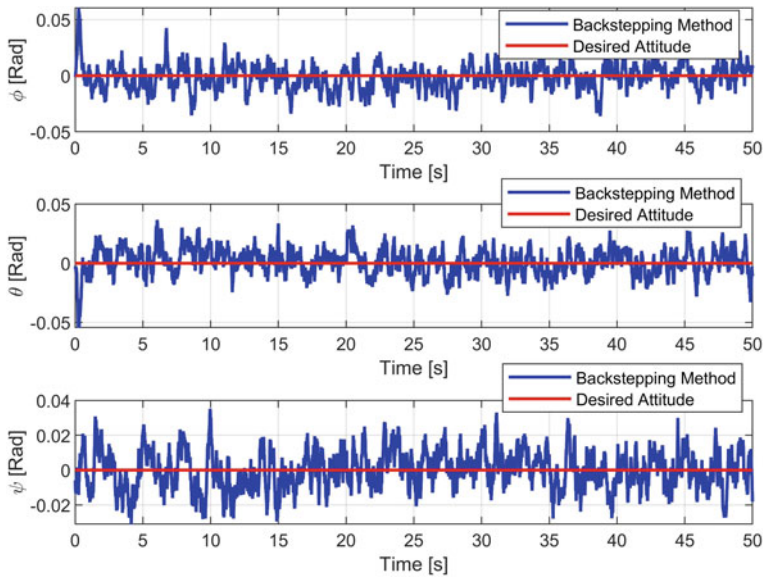
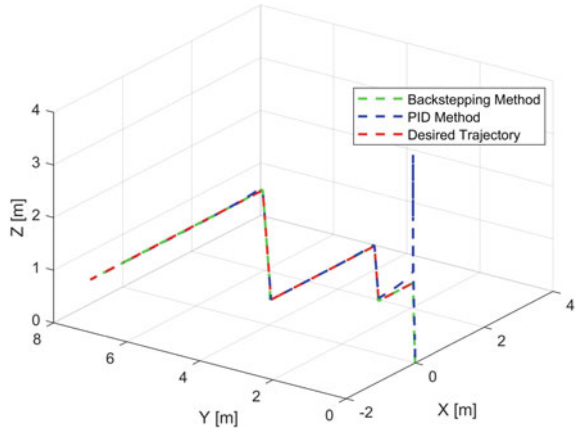


Fig. 4 Attitude of the UAV of Exp1: Spatial el-lipse with horizontal attitude (with noise)

Fig. 5 Spatial trajectory of the UAV of Exp2: Zigzag with horizontal attitude by applying Backstepping or PID



$$\underbrace{\begin{cases} x_d = 1 \\ y_d = 1 \\ z_d = 1 \end{cases}}_{t \in (0, 5s]} \Rightarrow \underbrace{\begin{cases} x_d = -0.2t + 2 \\ y_d = 1 \\ z_d = 1 \end{cases}}_{t \in (5, 10s]} \dots \underbrace{\begin{cases} x_d = 0.4t - 13 \\ y_d = 0.4t - 9 \\ z_d = 1 \end{cases}}_{t \in (30, 40s]} \Rightarrow \underbrace{\begin{cases} x_d = -0.5t + 23 \\ y_d = 7 \\ z_d = 1 \end{cases}}_{t \in (40, 50s]} \quad (18)$$

The control coefficient $c_1 \sim c_6 = 10, c_7 \sim c_{12} = 4$. Figure 5 presents the fuselage spatial trajectory and Fig. 6 and 7 show the x, y, z coordinates and three attitude angles ϕ, θ, ψ , respectively.

Exp 2 also proves the reliability of our proposed method. The UAV can track along a series of straight lines while maintaining a horizontal attitude, which is also impossible for conventional rotorcrafts. Meanwhile, by comparing our method with the PID method, we can see that in the X and Y axis directions, the overshoot and convergence speed of our method is similar to the PID. In the Z axis direction, the overshoot of our method is much smaller than that of the PID method. In terms of attitude control, the overshoot of our method is less than PID and the response speed is faster than the latter. Overall, the control result of our method is better than the PID method, which proves the significance of our method.

4.3 Hovering with Changing Attitude by Applying Backstepping or PID

In this simulation, the UAV hovers at a point with changing attitude. Since we have given the assumption of small attitude angles, the range of attitude angles is relatively small. Meanwhile, this task cannot be conducted by conventional rotorcrafts, either. The initial position and attitude are $(0, 0, 0)m$ and $(0, 0, 0)rad$, respectively. The desired position is $(0, 0, 0)m$, and the desired attitude is presented as follows: $\phi_d =$

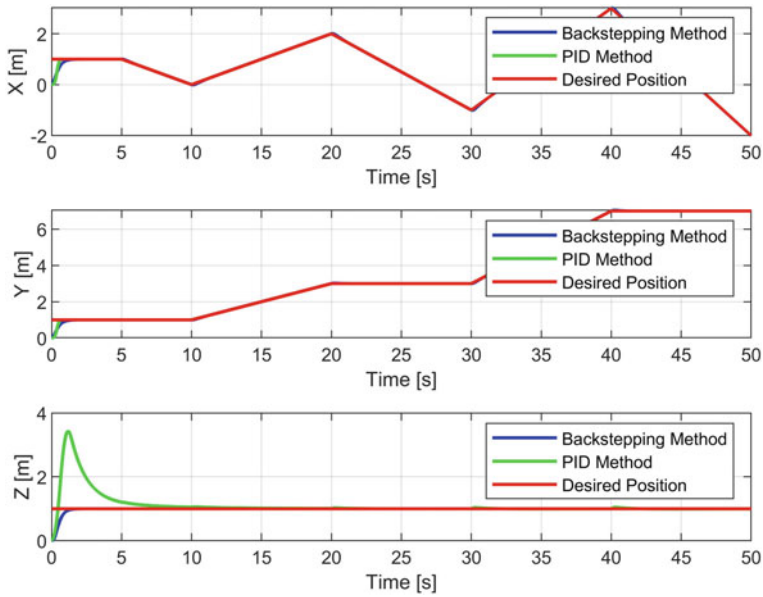


Fig. 6 Position of the UAV of Exp2: Zigzag with horizontal attitude by applying Backstepping or PID

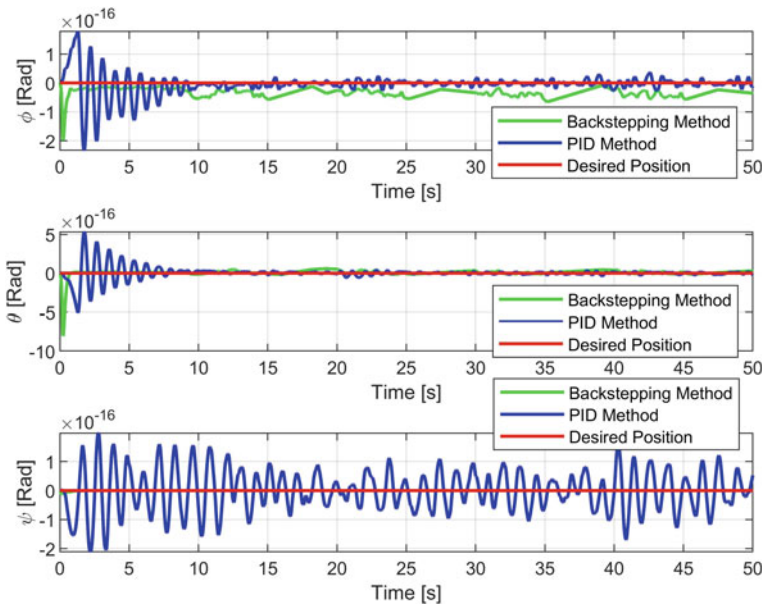


Fig. 7 Attitude of the UAV of Exp2: Zigzag with horizontal attitude by applying Backstepping or PID

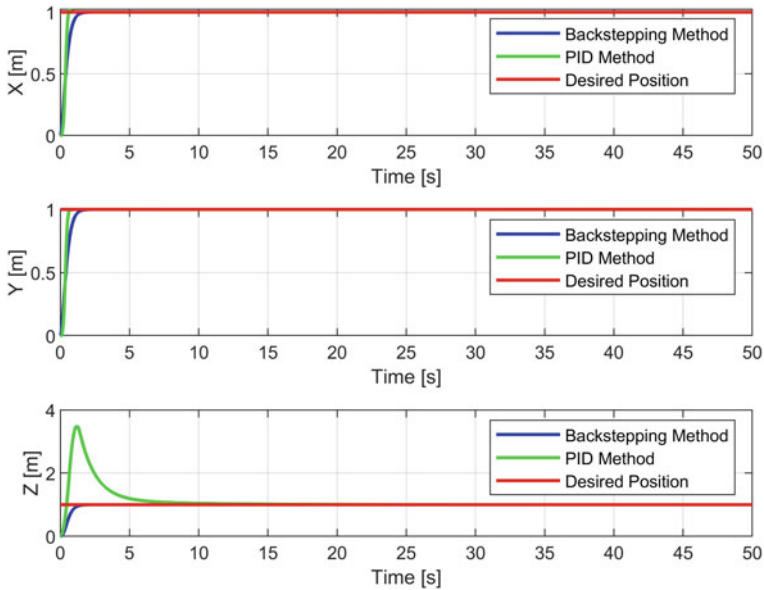


Fig. 8 Position of the UAV of Exp3: Hovering with changing attitude

$0.08 \cos(0.05\pi t)$, $\theta_d = 0.08 \sin(0.05\pi t)$, $\psi_d = 0.08$. The control coefficient $c_1 \sim c_6 = 6$, $c_7 \sim c_{12} = 3$. Figure 8 and 9 show the x , y , z coordinates and three attitude angles ϕ , θ , ψ , respectively. Herein, we apply the classic PID method for comparison as follows, $U_i = s_{i1}(x_{id} - x_i) + s_{i2} \int (x_{id} - x_i)dt + s_{i3}(\dot{x}_{id} - \dot{x}_i)$ ($i = 1, \dots, 6$)

where these coefficients can be chosen as follows: $s_{11} = s_{21} = 7500$, $s_{12} = s_{22} = 0$, $s_{13} = s_{23} = 1000$, $s_{31} = 20$, $s_{32} = 3$, $s_{33} = 20$, $s_{41} = s_{51} = 5.7$, $s_{42} = s_{52} = 1$, $s_{43} = s_{53} = 0.1$, $s_{61} = 7$, $s_{62} = 1.01$, $s_{63} = 0.15$.

Exp 3 is also a task that conventional rotorcrafts cannot accomplish. Similar to the results of Exp 2, our method has better overall control effect than PID method. At the same time, it can be noted that the Backstepping method we used is equipped with the assumption of small angle approximation, so the range of angles change we set here cannot be too large, otherwise the results will diverge.

5 Conclusion

In summary, a special structure fully-actuated tri-rotor UAV is introduced. Its control method and control allocator are both developed to make it more maneuverable. The proposed UAV complete many tasks that classical rotorcrafts cannot, which means the broad application prospects. Backstepping method we used here shows decent control effect, the control allocator solves the difficulty of non-linearity. Meanwhile,

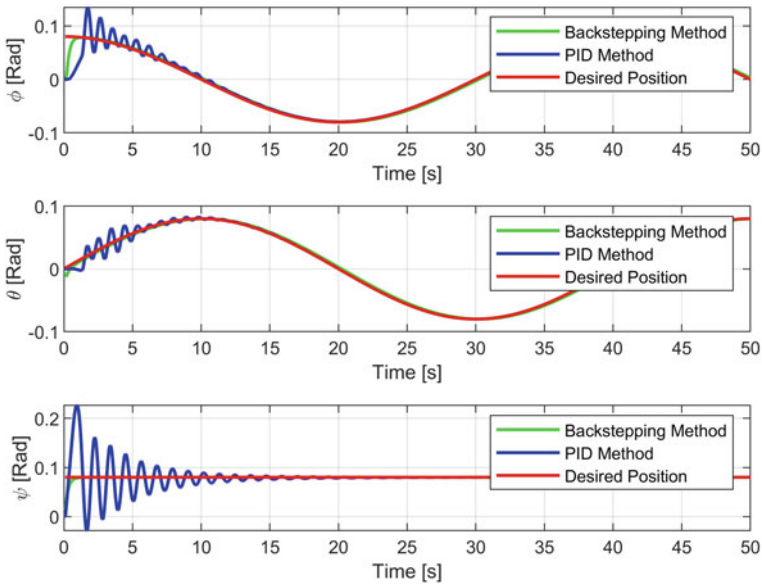


Fig. 9 Attitude of the UAV of Exp3: Hovering with changing attitude

actual flight tests will be conducted to validate the proposed UAV's reliability in future. Finally, a novel structure, such as an over-actuated tri-rotor will be developed to further improve UAV's mobility and potential.

Acknowledgements This work was supported by the National Natural Science Foundation of China (Grant No. 61673341), National Key R&D Program of China (2016YFD0200701-3), the Project of State Key Laboratory of Industrial Control Technology (Zhejiang University) (No. ICT1913) and the Open Research Project of the State Key Laboratory of Industrial Control Technology, Zhejiang University, China (No. ICT1900312).

References

1. Li, J., Li, Y.: Dynamic analysis and PID control for a quadrotor. In: 2011 IEEE International Conference on Mechatronics and Automation, pp. 573–578. IEEE (2011)
2. Xia, G.Y., Liu, Z.H.: Quadrotor unmanned helicopter attitude control based on improved ADRC. In: Proceedings of 2014 IEEE Chinese Guidance, Navigation and Control Conference, pp. 916–921. IEEE (2014)
3. Gadewadikar, J., Lewis, F., Subbarao, K., Chen, B.M.: Structured H-infinity command and control-loop design for unmanned helicopters. *J. Guidance Control Dyn* **31**(4), 1093–1102 (2008)
4. Song, Z., Li, K., Cai, Z., Wang, Y., Liu, N.: Modeling and maneuvering control for tri-copter based on the back-stepping method. In: 2016 IEEE Chinese Guidance, Navigation and Control Conference (CGNCC), pp. 889–894. IEEE (2016)

5. Lee, T., Leok, M., McClamroch, N.H.: Control of complex maneuvers for a quadrotor UAV using geometric methods on SE (3). arXiv preprint [arXiv:1003.2005](https://arxiv.org/abs/1003.2005) (2010)
6. Pratt, C.J., Leang, K.K.: Dynamic underactuated flying-walking (DUCK) robot. In: 2016 IEEE International Conference on Robotics and Automation (ICRA), pp. 3267–3274. IEEE (2016)
7. Brescianini, D., D’Andrea, R.: Design, modeling and control of an omni-directional aerial vehicle. In: 2016 IEEE international conference on robotics and automation (ICRA), pp. 3261–3266. IEEE (2016)
8. Segui-Gasco, P., Al-Rihani, Y., Shin, H.S., Savvaris, A.: A novel actuation concept for a multi rotor UAV. *J. Intell. Robot. Syst.* **74**(1–2), 173–191 (2014)
9. Şenkul, F., Altuğ, E.: Adaptive control of a tilt-roll rotor quadrotor UAV. In: 2014 International Conference on Unmanned Aircraft Systems (ICUAS), pp. 1132–1137. IEEE (2014)
10. Huang, H.: Control allocation of reaction control jets: quantization and stability. *J. Guidance Control Dyn.* **38**(1), 136–143 (2014)
11. Abdelmoeti, S., Carloni, R.: Robust control of UAVs using the parameter space approach. In: 2016 IEEE/RSJ International Conference on Intelligent Robots and Systems (IROS), pp. 5632–5637. IEEE (2016)
12. Boubdallah, S., Siegwart, R.: Backstepping and sliding-mode techniques applied to an indoor micro quadrotor [c]. *Proceedings of the 2005 IEEE Int. Conf. Robot. Autom.* IEEE, 2247–2252 (2005)
13. Alhardi, K.S.D.: Backstepping control and transforming of multi-output affine nonlinear systems into a strict feedback form [J] (2019)
14. Kamel, M., Verling, S., Elakhatib, O., et al.: The voliro omni orientational hexacopter: An agile and maneuverable tilttable-rator aerial vehicle [J]. *IEEE Robot. Autom. Mag.* **25**(4), 34–44 (2018)